CNRS - Université Pierre et Marie Curie - Université Versailles-Saint-Quentin
CEA - ORSTOM - Ecole Normale Supérieure - Ecole Polytechnique

Institut Pierre Simon Laplace

des Sciences de l'Environnement Global

Notes du Pôle de Modélisation

The Role of Lateral Ocean Physics in the Upper Ocean Thermal Balance of a Coupled Ocean-Atmosphere GCM

Eric Guilyardi (1), Gurvan Madec (2), and Laurent Terray (1)

(1) Centre Européen de Recherche et de Formation Avancée en Calcul Scientifique, Toulouse, France
(2) Laboratoire d'Océanographie DYnamique et de Climatologie (CNRS/UPMC/IRD), Paris, France

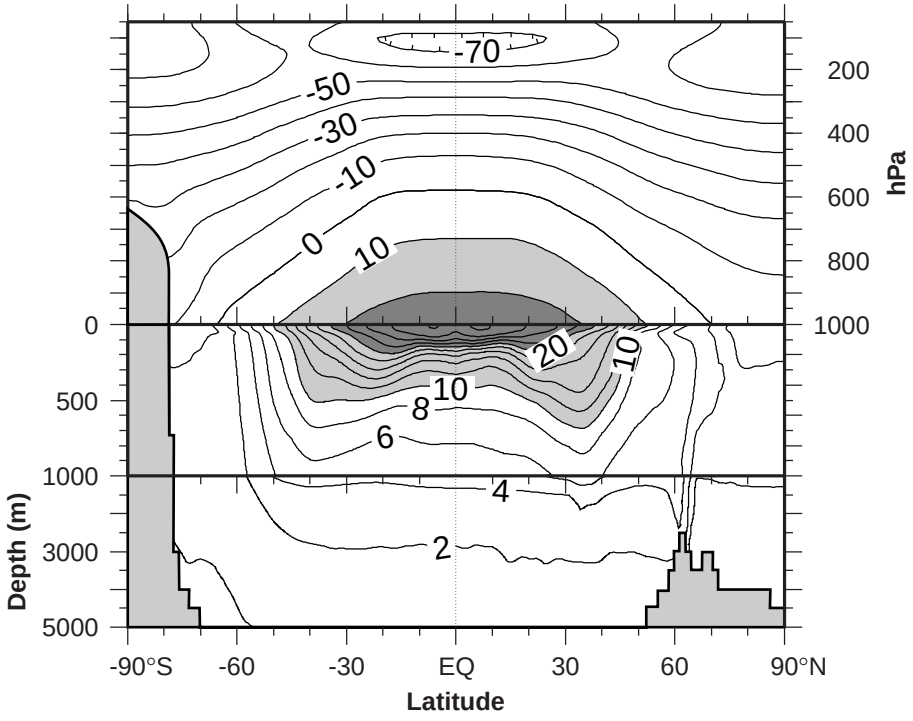

Février 1999 **Note n°13**

The Role of Lateral Ocean Physics in the Upper Ocean Thermal Balance of a Coupled Ocean-Atmosphere GCM

Eric Guilyardi [(1),] Gurvan Madec [(2),], and Laurent Terray [(1),]

(1) Centre Européen de Recherche et de Formation Avancée en Calcul Scientifique, Toulouse, France
(2) Laboratoire d'Océanographie DYnamique et de Climatologie (CNRS/UPMC/IRD), Paris, France

RÉSUMÉ

La sensibilité de l'équilibre thermique des couches de surface de l'océan à la physique latérale océanique est étudiée dans le système couplé OPA/OASIS/ARPEGE. Trois simulations couplées de 40 ans sont comparées. Elles utilisent respectivement pour physique latérale un mélange horizontal, isopycnal, et isopycnal plus une advection induite par les tourbillons. L'ajustement thermique du système couplé est très différent suivant les simulations, confirmant le rôle majeur du mélange latéral océanique dans l'équilibre climatique. Les différences les plus importantes se manifestent en terme d'augmentation de température de surface océanique aux moyennes latitudes, en particulier dans l'hémisphère sud. Un bilan de chaleur dans le "bol" (i.e. la partie de l'océan superficiel au moins mélangé verticalement une fois dans l'année) montre que ces changements proviennent d'une modification des échanges entre le "bol" et l'océan intérieur. Comparé au mélange horizontal, le mélange isopycnal extrait plus efficacement de la chaleur de l'océan intérieur. Cet échange de chaleur est maximum en hiver et résulte de: (1) l'accroissement de la surface effective de diffusion due à l'inclinaison de la direction de mélange, et (2) la présence d'eau plus chaude mais plus salée à la base du "bol" que dans le "bol" lui-même.

Ces simulations mettent donc en évidence le rôle clé de la structure haline dans l'équilibre thermique de l'océan. La présence du sel contôle la manière dont la chaleur est extraite de l'océan intérieur: Sans sel, isopycnes et isothermes se confonderaient annulant le flux diffusif. L'ajout d'une advection induite par les tourbillons a un effet similaire, là encore associé à la structure haline de l'océan. Il rend encore plus efficace l'extraction de chaleur de l'océan intérieur par la physique latérale.

Note du Pôle de modélisation, Février 1999, N°13
Directeur de publication : Gérard Mégie, directeur de l'IPSL

ISSN 1288-1619

The Role of Lateral Ocean Physics in the Upper Ocean Thermal Balance of a Coupled Ocean-Atmosphere GCM

ERIC GUILYARDI[1*], GURVAN MADEC[2] AND LAURENT TERRAY[1]

1. Centre Européen de Recherche et de Formation Avancée en Calcul Scientifique, Toulouse, France
2. Laboratoire d'Océanographie Dynamique et de Climatologie (CNRS/UPMC/IRD), Paris, France

ABSTRACT

The sensitivity of the upper ocean thermal balance of the OPA/OASIS/ARPEGE coupled GCM to lateral ocean physics is assessed. Three 40-year simulations are performed using horizontal mixing, isopycnal mixing, and isopycnal mixing plus eddy-induced advection. The isopycnal-only mixing is used with no horizontal background diffusion and thus refered as "pure". The thermal adjustment of the coupled system is quite different between the simulations, confirming the major role of ocean mixing on the heat balance of climate. The initial adjustment phase of the upper ocean (SST) is used to diagnose the physical mechanisms involved in each parameterisation. When the lateral ocean physics is modified, significant changes of SST are seen, mainly in the southern ocean. A heat budget of the annual mixed layer (defined as the "bowl") shows that these changes are due to a modified heat transfer between the bowl and the ocean interior. This modified heat intake of the ocean interior is directly due to the added physics. In isopycnal diffusion, this heat exchange, especially marked at mid-latitudes, is both due to an increased effective surface of diffusion and to the sign of the isopycnal gradients of temperature at the base of the bowl. As this gradient is proportional to the isopycnal gradient of salinity, this confirms the quite strong role of salinity in the thermal balance of the coupled system. The eddy-induced advection also leads to increased exchanges between the bowl and the ocean interior. This is both due to the shape of the bowl and again to the existence of a salinity structure. The lateral ocean physics is shown to be a significant contributor to the exchanges between the diabatic and the adiabatic parts of the ocean.

1. Introduction

Due to its high thermal inertia and to its opacity, the ocean stores vast amounts of energy, away from a direct contact with the atmosphere. As part of the gigantic thermodynamical machine of climate, the ocean acts as a heat regulator. This regulation involves both air-sea (and ice-sea) heat exchanges and mixing within the ocean. It is therefore closely related to the internal structure of the ocean: water masses are *formed* in the surface diabatic region of the ocean, are advected adiabatically, and are finally *consumed* by the only diabatic process within the ocean: turbulent mixing. Here, we wish to assess the sensitivity of the climate modeled by a coupled ocean-atmosphere GCM to the representation of such ocean physics. The particular focus of this paper is on the role of the lateral ocean physics on the thermal balance of the upper ocean.

Classical views of the thermocline ventilation (Luyten *et al.* 1983) propose a theoretical framework to explain the observed density structure at mid-latitudes. This advective approach has proven successful in several regions of the ocean (Luyten *et al.* 1983, Rhines and Young 1982, Marshall and Nurser 1992). Nevertheless, air-sea fluxes are usually not taken into account explicitly but through the specification of the density at the base of the mixed-layer. In addition, mixing is usually neglected because considered small. Tziperman (1986) showed that these two simplifications are intimately related. He re-introduces mixing by showing that *however small*, it has a major role in the equilibrium of the thermocline. The basic physical idea underlying this approach (Walin 1982) is quite simple: air-sea implied buoyancy can generate a *net* water volume of a particular density class ρ. If the ocean is close enough to a statistically steady state, there must be a counter-balancing interior diapycnal mixing. Difficult to measure, long neglected in theoretical works, ocean turbulent mixing rates are little known. Their climatic importance has motivated a renewed interest (Gargett 1989, Caldwell and Moum 1995) and recent in-situ experiments are shedding some light on processes in specific regions of the ocean (Ledwell *et al.* 1993, 1998, Toole *et al.* 1994, Polzin *et al.* 1996, 1997), modifying the classical views of mixing into more complex schemes.

Due to the lack of observations on the global space and climate time scales, numerical modeling, as a test case for theory, is required to tackle these issues. Numerical ocean general circulation models (OGCM) are based on primitive equations. Because of the coarse grids used in climate simulations, they perform a space and

Corresponding author address: Dr. Eric Guilyardi, LODYC, case 100, 4 place Jussieu, 75252 Paris Cedex 05, France
E-mail: ericg@lodyc.jussieu.fr

time filter of the flow. Hence, sub-grid-scale (SGS) physical processes, including turbulent mixing, need to be parameterized. This requirement is probably the most challenging issue in climate OGCMs as: 1) mixing is difficult to measure and no validation is possible on global/climate time scales, 2) SGS physics has to be a function of the larger-scale prognostic quantities and 3) numerical stability often requires artificial diffusion. The classical parameterisation of ocean mixing is of fickian type, where SGS fluxes act simply to mix the mean field for some large-scale property τ (with a down-gradient flux $K\nabla\tau$). On the vertical, this form of mixing usually models both the ocean interior diapycnal mixing and the downward penetration of the wind and buoyancy driven circulation. Because of the marked mixing regimes on the vertical, the issue is then which K_v to choose (see review by Large *et al.* 1994). Eddies in the ocean further mix tracers along isopycnals. Even though less justified on tracers, fickian type lateral eddy fluxes are still widely used to model this effect in climate models (which do not explicitly resolve these mesoscale eddies). In this case the issue is not only which diffusion coefficient K_l to choose but also the orientation of the tensor: horizontal or along isopycnals (Redi 1982, Cox 1987). Breaking the all-fickian formulation, alternative parameterisations of the effect of eddies have been proposed, in particular to take into account the loss of mean potential energy by baroclinic instability (Gent and McWilliams 1990, McDougall and McIntosh 1996, Killworth 1997).

Many sensitivity studies show that the modeled ocean is highly sensitive to the representation of mixing (England 1993, Hirst and Cai 1994, Danabasoglu and McWilliams 1995, Maes *et al.* 97, England and Hirst 1997, see review by McWilliams 1996). All these studies have been made in forced mode, where the ocean mixed layer is constrained by a surface restoring to observed temperature and salinity. In the present sensitivity study we choose to couple the ocean GCM to an atmosphere GCM. Several reasons motivate this choice. First, the mixed layer is now free to adjust to the atmosphere; this yields more consistent boundary conditions, and hence air-sea fluxes. Second, the energy budget of the ocean-atmosphere thermodynamical machine is closed and can be used to diagnose the heat regulation role of the ocean. Last but not least, *a free mixed layer allows the physics to express itself*: a change of mixing scheme will affect the consumption of water masses and, following Walin's idea, will consequently modify their formation, hence the air-sea fluxes. In forced mode, the surface constraint specifies the outcrops of the density/temperature field and therefore affects the physics of the mixed-layer: its buoyancy balance is inconsistent as the interior diapycnal exchanges can have inconsistent feedbacks on the patterns of the surface forcing. This is especially true in strong gradients regions (west-borders currents, fronts), where a slight geographical shift of the modeled gradients leads to unrealistically large heat and fresh water restoring fluxes. These terms, while keeping surface characteristics close to the climatology, hence represent significant and questionable sources of water-masses in key regions. In coupled mode, the atmosphere is part of the feedback loop and air-sea fluxes can adjust to the new ocean physics and the associated surface gradients. Following the same approach, the analysis of the coupled simulations is made using the initial adjustment phase (away from its observed initial state) where the "work" of the physical parameterisation is particularly visible. In addition, understanding this departure from the observed (a classical bias of coupled models) will help reduce it and finally improve the model. This strategy allows short simulations (several decades) and keeps reasonable the computer requirements (an obvious downside of coupled GCMs). In this study, we assess the sensitivity of the modeled climate to the lateral ocean physics on tracers, and in particular the role of lateral mixing on the bowl — ocean interior exchanges. Three 40-year coupled simulations are made using horizontal mixing, isopycnal mixing, and isopycnal mixing plus eddy-induced advection, respectively.

The paper is organized as follows. Section 2 describes the coupled model and the sensitivity experiments. Section 3 compares the response of the three simulations with special emphasis on the air-sea interface. Section 4 focuses on the physical mechanisms involved in the exchanges between the bowl and the ocean interior. The climatic impact of these differences are discussed in section 5 and we conclude the paper in section 6 with a summary and some directions for future work.

2. The OPA/OASIS/ARPEGE coupled model

2.a The OPA model

The OPA8 ocean GCM has been developed at the Laboratoire d'Océanographie DYnamique et de Climatologie (LODYC) (Madec *et al.* 1997). It solves the primitive equations with a non-linear equation of state (Unesco 1983). A rigid lid is assumed at the sea surface. The code has been adapted to the global ocean by Madec and Imbard (1996). The horizontal mesh is orthogonal and curvilinear on the sphere. It does not have a geographical configuration: the northern point of convergence has been shifted onto Asia to overcome the singularity at the North Pole (Madec and Imbard 1996). Its space resolution is roughly equivalent to a geographical mesh of 2 by 1.5 degrees (with a meridional resolution of 0.5° near the Equator). 31 vertical levels are used with 10 levels in the top 100 meters (Madec and Imbard 1996). The model time step is 1h40'. Vertical eddy diffusivity and viscosity coefficients are computed from a 1.5 turbulent closure scheme (Blanke

and Delecluse 1993) which allows an explicit formulation of the mixed layer as well as minimum diffusion in the thermocline (the minimum background value is set to $10^{-5} m^2 s^{-1}$ following Ledwell *et al.* 1997). The solar radiation is allowed to penetrate in the top meters of the ocean (Blanke and Delecluse 1993). Zero fluxes of heat and salt and no-slip conditions are applied at solid boundaries. Sea-ice is restored towards observations at high latitudes. Horizontal mixing of momentum is of fickian type with an eddy viscosity coefficient of $4.10^4 m^2 s^{-1}$, reduced in the Tropics to reach $2.10^3 m^2 s^{-1}$ at the Equator. The lateral mixing on tracers (temperature and salinity), on which the sensitivity experiment is performed, is described in section 2.d.

2.b The ARPEGE model

The ARPEGE-climat (Version 2) atmosphere GCM, from CNRM/Météo-France, is a state of the art spectral atmosphere model developed from the ARPEGE/IFS weather forecast model (Déqué *et al.* 1994). The ARPEGE model used in this study is based on the version described by Guilyardi and Madec (1997) with the following differences. The model now has 19 vertical levels (with an increased resolution in the troposphere) and a triangular spectral T31 truncation is used for horizontal resolution corresponding to a 3.75° grid size. The convective entrainment rate is increased at lower levels, the radiation scheme is now based on the Fouquart-Morcrette scheme described in Dandin and Morcrette (1996) and, following Terray (1998), a parameterisation of marine strato-cumulus is added. These last three modifications clearly improved the tropical climatology of the coupled model when compared to that of Guilyardi and Madec (1997). In particular, the strong initial tropical warming was strongly reduced (see Guilyardi 1997 for a full discussion). Finally, a 4-layer prognostic soil scheme with seasonally varying surface albedo is added as well as a new parameterisation of gravity-wave drag.

2.c Coupling procedure and initialization

The coupling procedure is similar to the one described in Guilyardi and Madec (1997): synchronous coupling with a daily exchange of fluxes. The version 2.0 of OASIS is used (Terray *et al.* 1996) in which the SST of a given AGCM grid square is now the weighted average of the underlying OGCM sea grid points. The river runoffs are computed using 81 river drainage basins defined on the AGCM grid and are passed instantaneously to corresponding river mouth ocean grid points. As the analysis of the initial adjustment phase is the topic of this paper, the initial state of the ocean is based on the atlas of Levitus (1982) followed by a short dynamic spin-up (Madec and Imbard 1996, Guilyardi and Madec 1997), and no artificial flux corrections are applied at the air-sea interface (except in sea-ice regions).

2.d The 3 sensitivity experiments

Based on the coupled model described above, a sensitivity study to ocean lateral diffusion of tracer is made. The reference experiment (**HOR**) is integrated for 40 years. It uses a classical horizontal harmonic diffusion scheme (Fig. 1-a), with an eddy diffusivity coefficient K_H of $2.10^3 m^2 s^{-1}$. As noted by many authors, this horizontal diffusion scheme generates spurious diapycnal fluxes where the isopycnals are steeply sloping. Redi (1982) and Cox (1987) introduced a scheme in which harmonic diffusion acts along isopycnal surfaces (in fact, along neutral surfaces — McDougall 1987) (Fig. 1-b). The Cox implementation of isopycnal diffusion in GFDL-type models nevertheless requires a minimum background horizontal diffusion for numerical stability. To overcome this problem, several techniques have been proposed in which the numerical schemes of the OGCM are modified (Griffies *et al.* 1997, Weaver and Eby 1997). In OPA, another strategy has been chosen: a local horizontal filtering of the isopycnals slope is made prior to the computation of the isopycnal diffusion operator. This prevents the development of grid-point noise so that no artificial background horizontal mixing has to be added (thus allowing "pure" isopycnal mixing). A 40-year coupled simulation is performed using the OPA "pure" isopycnal diffusion scheme (experiment **ISO**) with an eddy diffusivity coefficient K_L of $2.10^3 m^2 s^{-1}$.

Baroclinic instability is a significant source of mixing within the ocean. It induces a loss of mean potential energy which is nevertheless not affected by the horizontal or the isopycnal diffusion operators. In order to mimic this process, Gent and McWilliams (1990, GM90 thereafter) proposed a quasi-adiabatic parameterisation in which an eddy-induced advection is added to the tracer equation (Gent *et al.* 1995). This eddy-induced velocity (EIV) represents the ageostrophic part of the motion (Lazar et al. 1999), in the sense that it is not in equilibrium with a pressure gradient, even though the eddies modeled (because not resolved by climate models) may be geostrophic. The eddy-induced velocity proposed by GM90 is proportional to the gradient

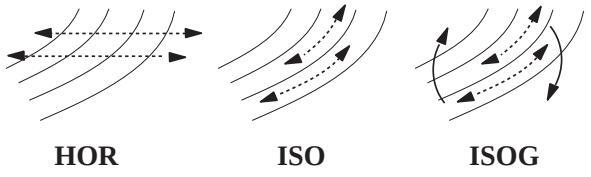

FIG. 1. *The 3 lateral diffusion parameterisations used in this study.* ***HOR*** *horizontal diffusion,* ***ISO*** *isopycnal diffusion and* ***ISOG*** *isopycnal diffusion plus eddy-induced velocity (see text). Isocontours represent the neutral density field.*

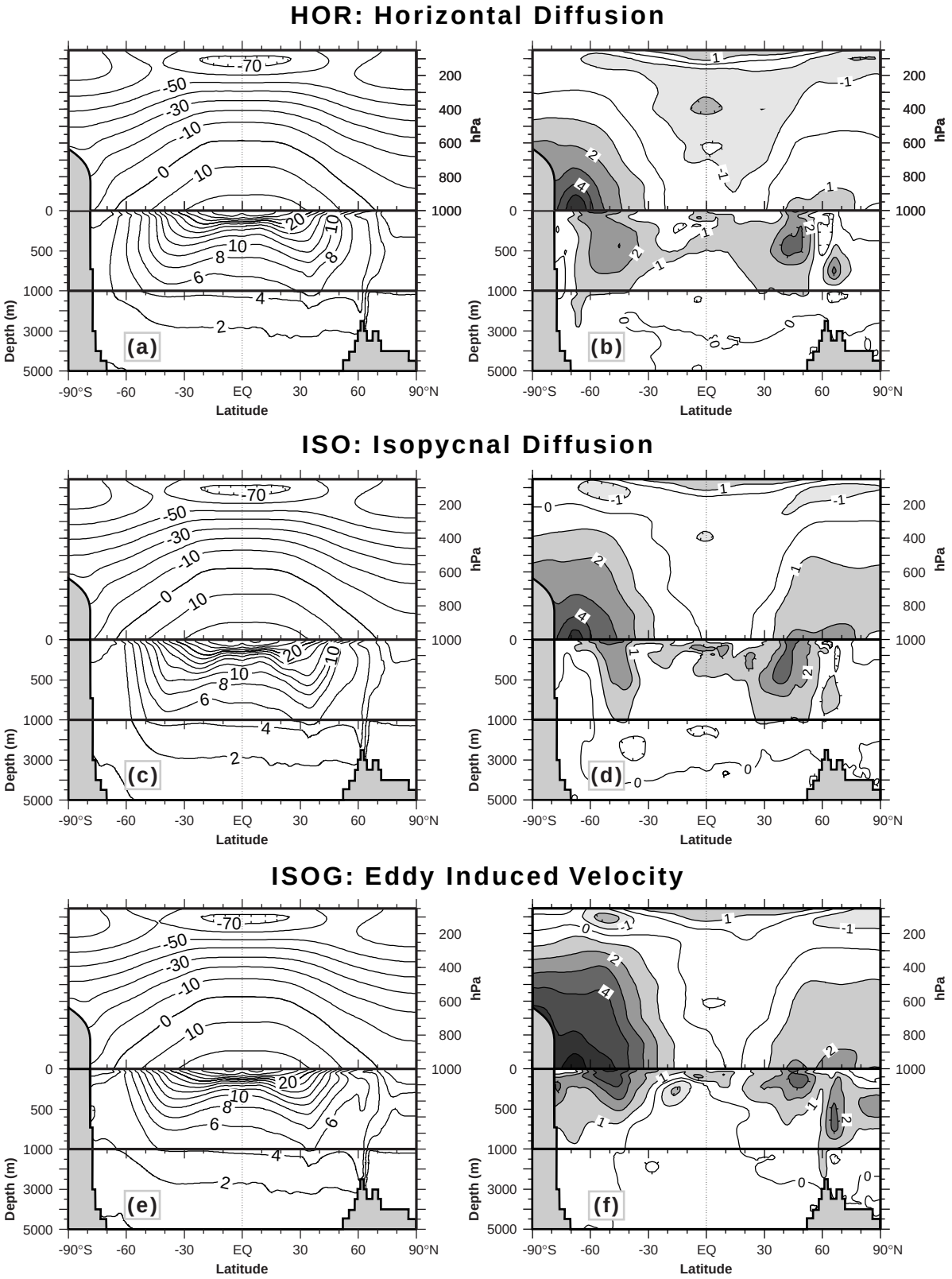

FIG. 2. *Zonal mean temperature (°C) in the coupled ocean-atmosphere system. Average of years 26-40. (a) simulation **HOR**, (c) simulation **ISO**, (e) simulation **ISOG**, (b), (d), (f): differences with the initial state of each simulations. Contour interval 10°C in the atmosphere, 2°C in the ocean and 1°C in the difference figures.*

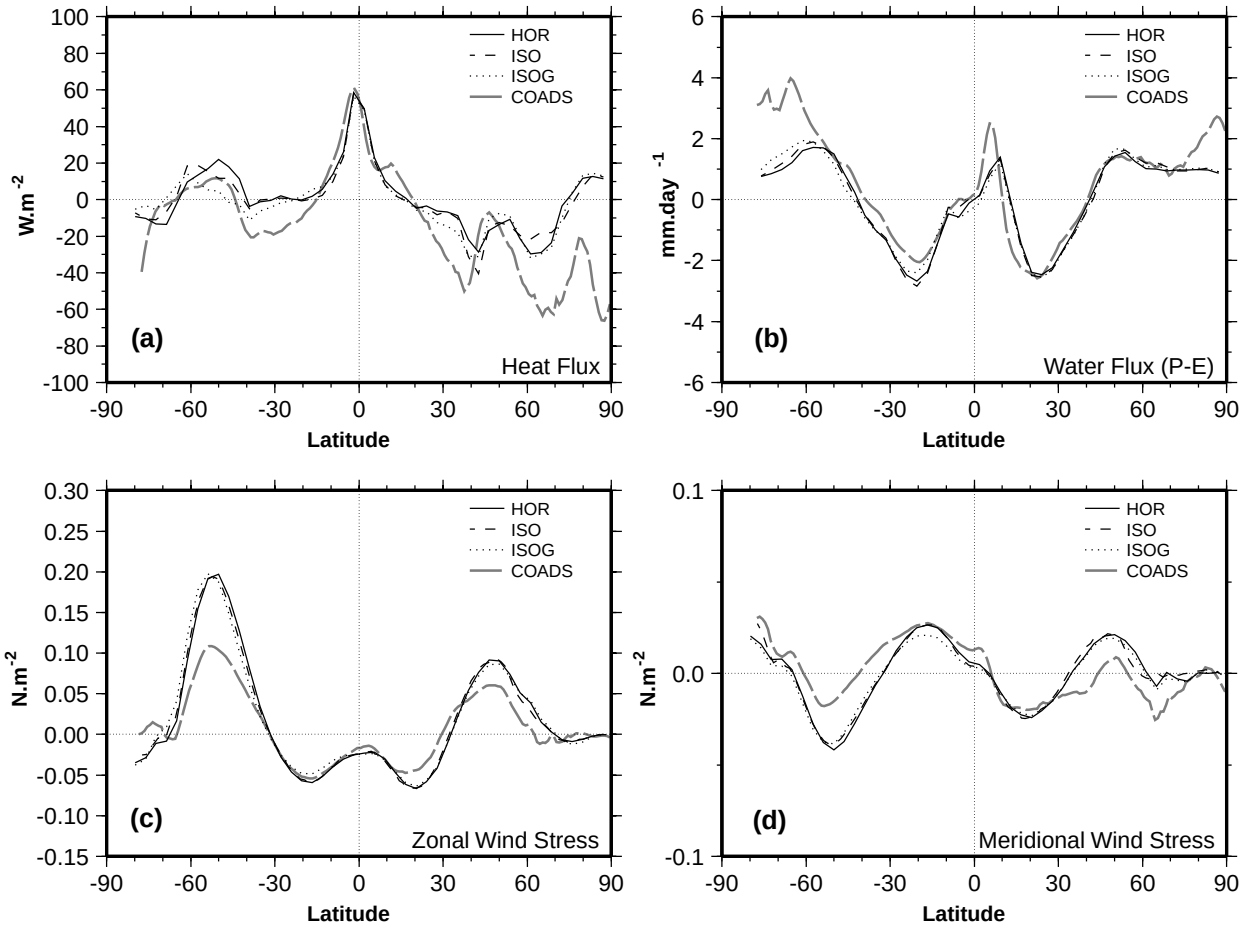

FIG. 3. *Zonal mean of air-sea fluxes. Average of years 26-40 for simulations; COADS climatology by Da Silva* et al. *(1996). (a) downward heat flux, (b) fresh water flux P-E, (c) zonal wind stress and (d) meridional wind stress.*

of the slope of the isopycnal ($U^* = K_{eiv} \nabla \cdot [\text{slope}]$) and therefore tends to slump density fronts (Fig. 1-c). The third 40-year simulation (experiment **ISOG**) includes such an eddy-induced advection, in addition to the isopycnal diffusion, with $K_{eiv} = K_I = 2.10^3 m^2 s^{-1}$. This value of K_{eiv} is quite high for most ocean regions when compared to those estimated in the literature (Visbeck *et al*. 1997). It is nevertheless kept to $2.10^3 m^2 s^{-1}$ to magnify its effect in the model. The surface boundary condition of U^* was not discussed by GM90 and is not straightforward to choose (Tréguier *et al.* 1997, Marshall 1997, Killworth 1997). In this first implementation of GM90 in OPA, the slopes are bounded by 1/100 everywhere, this limit linearly decreasing to zero between 70 meters depth and the surface (the fact that eddies "feel" the surface motivates this flattening of isopycnals near the surface).

3. The coupled response

This section briefly describes the main differences between the 3 simulations, with a special emphasis on the initial adjustment phase of the air-sea interface. A more detailed assessment of the compared climatology of the 3 simulations can be found in Guilyardi (1997)

The zonal mean temperature evolution in the atmosphere after 40 years presents a similar pattern for the three simulations (Fig. 2-b,d,f): tropical tropospheric cooling associated to a warming at higher latitudes, especially marked in the southern hemisphere. Nevertheless, the magnitude of the temperature drift is significantly affected by the changes in lateral ocean physics (roughly +2°C in the near surface layers from **HOR** to **ISOG** around 60°S). In contrast, the change of lateral ocean physics only very slightly affected the dynamics of the atmosphere: similar SST gradients led to similar pressure patterns and the dynamical forcing of the ocean (i.e Ekman pumping) is quite comparable between the 3 simulations (not shown). In the ocean, the 1.5 turbulent closure scheme maintains the sharp tropical thermocline and the marked **W** structure in all experiments (Fig. 2-a,c,e). At mid-latitudes, the shape of the isotherms is clearly affected by the lateral physics. For instance, between 40°S and 60°S, the isotherms in **HOR** are drawn poleward in the first 1000 m (Fig. 2-a) while their initial structure (front associated to the Antarctic Circumpolar Current) is preserved in **ISO** (Fig. 2-c) (the same effect on salinity maintains the Antarctic Intermediate Water salinity minimum in **ISO** which was diffused away in **HOR** —

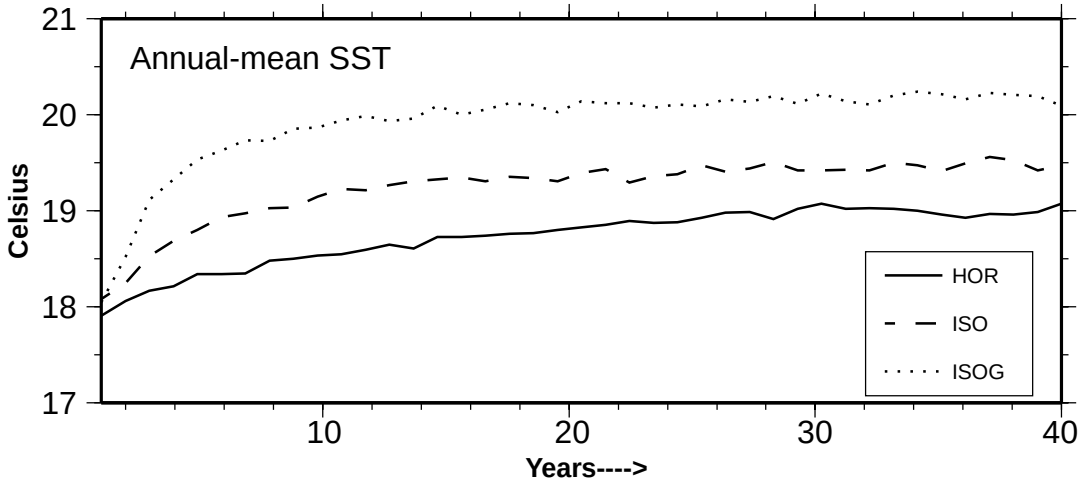

FIG. 4. *Time evolution of the annual-mean global SST (°C) for the 3 simulations.*

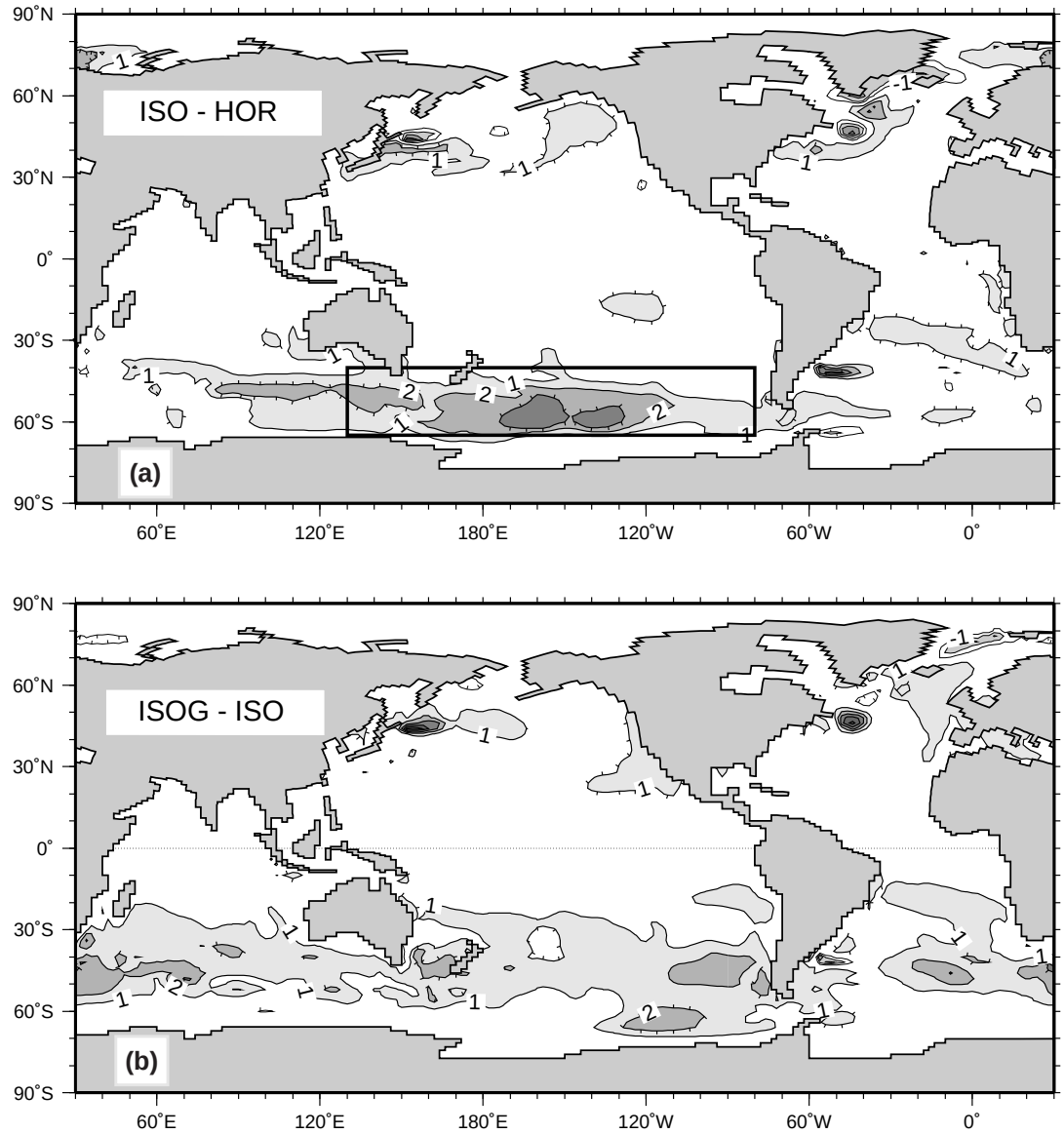

FIG. 5. *SST differences for year 03 (°C). (a)* ***ISO*** *minu* ***HOR*** *and (b)* ***ISOG*** *minus* ***ISO****. Contour interval 1°C.*

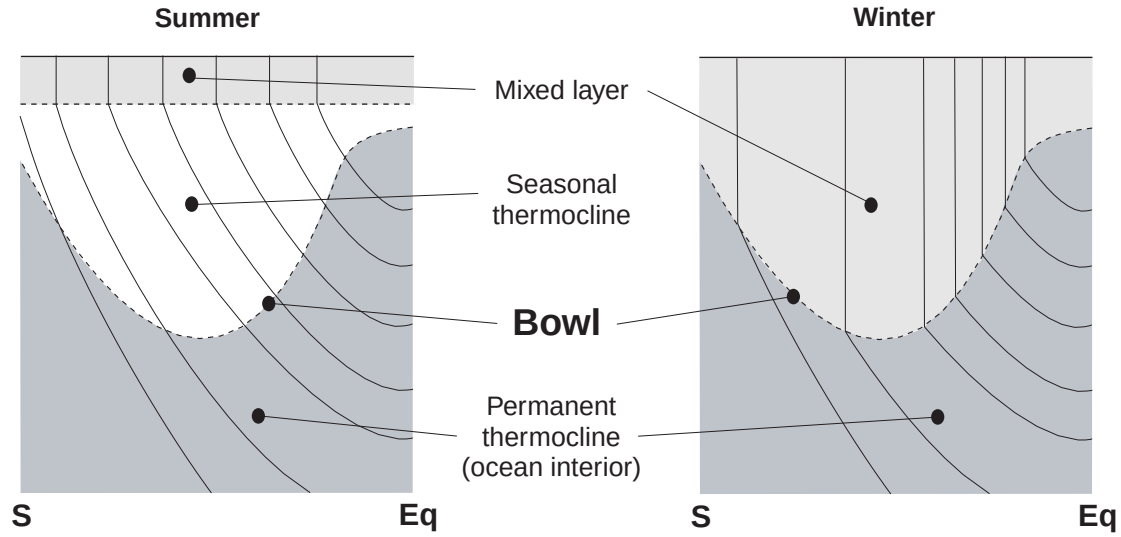

FIG. 6. *Definition of the "bowl", annual envelop of the mixed-layer (thick dashed line). The isocontours represent the density field. The bowl is fixed in time and allows a clear distinction of the diabatic and adiabatic parts of the ocean.*

not shown). In **ISOG**, an excessive slumping of the initial horizontal fronts is clearly visible at most latitudes, associated to an increased stratification at the base of the mixed layer (Fig. 2-e). On the difference plots, the excess of heat entering the southern ocean near 50°S is diffused horizontally in **HOR** (Fig. 2-b) while it remains along isotherms (isopycnals) in **ISO** (Fig. 2-d), diving to 1000m. In **ISOG**, the warming signal is shallower (600m deep at 45°S) and is spread in the surface layers by the slumping of the meridional fronts (Fig. 2-f).

The zonal mean heat flux, fresh water flux and wind stress components of **HOR**, **ISO** and **ISOG** displayed in Fig. 3 are quite close to each other when compared to climatology. The main common bias are extra-tropical: higher-than-observed heat fluxes entering the ocean at mid-latitudes (Fig. 3-a) (mostly due to a lack of clouds and deficient turbulent fluxes in the atmosphere GCM) and quite strong westerlies, especially over the southern ocean (Fig. 3-c). Most of the differences between the 3 simulations are found south of 40°S. They mainly concern the heat flux entering the ocean (which diminishes between 40°S and 60°S from **HOR** to **ISO** and to **ISOG**) while the fresh water flux and wind stress undergo very little changes.

The annual-mean SST of all 3 simulations increases from their common initial state (Fig. 4). This common feature is due to the atmosphere GCM deficiency discussed above, which generates higher-than-observed heat flux for most extra-tropical latitudes (Fig. 3-a). Nevertheless, the *amplitude* and the *time scale* of the SST warming are strongly affected by the change in lateral ocean physics: the annual-mean SST of **HOR** increases slowly but steadily while the initial increase in **ISO** is much stronger but reaches a quasi-equilibrium for the last 20 years of the simulation (Fig. 4). The annual-mean SST of **ISOG** exhibit the same behavior as the one of **ISO**, the initial warming during the first 3 to 5 years being even stronger. Global SST differences after 40 years are close to 1°C, suggesting significant changes in the initial thermal adjustment of the coupled model.

Difference maps after 3 years show that most of the SST differences occur at mid-latitudes, where the isopycnal have the strongest slope (Fig. 5). In particular, the SST warming from **HOR** to **ISO**, and further from **ISO** to **ISOG**, mostly takes place in the southern ocean where differences up to 3°C are locally seen (Fig. 5-a). After 40 years, the patterns and amplitude of SST differences are similar to the first 3 years (not shown), as expected from Fig. 4. A first candidate to account for these SST differences is a change of downward heat flux at the air-sea interface. The net heat fluxes entering the ocean for years 01-02-03 for **HOR**, **ISO** and **ISOG**, are *7*, *5.5* and *4* $W\,m^{-2}$, respectively (these figures stabilizing to *4.2*, *3.5* and *1.5* $W\,m^{-2}$, respectively, after 40 years). This indicates that the heat flux is not responsible for the SST increase from one simulation to the other. On the opposite, this reduced heat flux, mostly due to the latent heat flux (not shown) and located in the southern ocean (Fig. 3-a) is actually a *response* to the increase of SST. Hence, the heat required to increase the SST from **HOR** to **ISO** and further from **ISO** to **ISOG** must come from the ocean interior: an investigation of the thermal balance in the ocean is needed.

4. The heat balance of the bowl

The SST is, to a very good approximation, the temperature of the ocean mixed layer. Hence, in order to understand the SST differences described above, we need to assess the heat balance of the mixed layer. We first define the bowl as the annual envelop of the mixed

layer. An integration of the bowl temperature trends then shows that the SST changes from one simulation to the other directly come from the modified lateral ocean physics.

4.a The bowl, annual integrator of the air-sea fluxes

During the year, the mixed layer shallows and deepens, sweeping the *diabatic* region of the ocean while integrating the air-sea fluxes. We define the lower boundary of this region to be the thermodynamical "bowl", following the dynamical bowl discussed by Marshall and Nurser (1992). This annual envelop of the mixed layer is *fixed in time* and represent the boundary between the diabatic and adiabatic regions of the ocean (Fig. 6). The annual heat exchanges between these two regions of the ocean have to be computed through this surface rather than through the base of the mixed layer. Indeed, in summer, the mixed layer is shallow but the fluxes injected during the previous winter continue to interact with the ocean interior: the resulting waters (part of the seasonal thermocline, Fig. 6) are re-entrained in the mixed-layer the next winter and need therefore to be taken into account in the annual heat budget. In fact, the bowl represents an *annually integrated mixed layer* which allows to filter the seasonal cycle in the analysis of the heat exchanges between the atmosphere, the mixed layer and the ocean interior (see also Marshall *et al.* 1998).

The mixed layer used to define the bowl for each simulation is computed using a thermodynamical criterion on density ($\rho < \rho_0 + 0.01$, where ρ_0 is the surface density) rather than a dynamical criterion built on the intensity of the vertical mixing ("turbocline"). The bowl is then defined for each simulation as the maximum depth reached by the mixed layer over the study period (here years 01-02-03). In the remainder of the paper, the bowl is to be understood as the *volume* between the surface and the bowl defined above.

4.b Heat balance computation

The different trends driving the temperature equation in the bowl are vertically integrated at each time step for the first 3 years of each simulation, leading to the following equation:

$$\frac{\partial T_{bowl}}{\partial t} = \mathbf{Adv} + \mathbf{Forc} + \mathbf{SGS}$$

where $T_{bowl} = 1/H \int_{-H}^{0} T\, dz$ is the bowl temperature, H being the depth of the bowl, **Adv** is the advective trend, **Forc** is the trend due to the forcing (air-sea fluxes) and {\bf SGS} is the trend associated to sub-grid-scale processes. This last term includes the trends due to the lateral diffusion $\mathbf{Diff}_L$ (horizontal for **HOR** and isopycnal for **ISO** and **ISOG**), the vertical diffusion $\mathbf{Diff}_V$ and, for **ISOG**, to the eddy-induced velocity $\mathbf{Adv}_{EIV}$.

*TABLE 1. Bowl temperature trends (°C/year) integrated for years 01-02-03 of simulations in the region 130°E-80°W/40°S-65°S, and differences. $\partial_t T_{bowl}$ is the total trend; **Forc**, the forcing trend; **Adv** the advection trend; $\mathbf{Diff}_L$ and $\mathbf{Diff}_V$ the lateral and vertical diffusion trends and $\mathbf{Adv}_{EIV}$ the eddy-induced advection trend.*

°C/year (01-02-03)	**HOR**	**ISO**	**ISOG**	**ISO -HOR**	**ISOG -ISO**
$\partial_t T_{bowl}$	0.17	0.47	0.75	0.30	0.28
Forc	1.03	0.96	0.74	-0.07	-0.22
Adv	-1.03	-1.25	-1.72	-0.22	-0.47
$\mathbf{Diff}_L$	0.10	0.74	0.69	**0.64**	-0.05
$\mathbf{Diff}_V$	0.07	0.02	-0.02	-0.05	-0.04
$\mathbf{Adv}_{EIV}$	—	—	1.06	—	**1.06**

The cumulated trends in a southern region located where the difference maxima between the simulations occur (box 130°E-80°W/40°S-65°S drawn in Fig. 5-a) are presented for the 3 simulations and for the 3 first years in Table 1.

The basic balance in **HOR** at this latitude is between the forcing (warming, Fig. 3-a) and the advection (cooling by Ekman drift, Fig. 3-c), the other terms being small (Table 1). In **ISO**, the increase of T_{bowl} (+0.3 °C/year when compared to **HOR**) is solely due to the lateral diffusion $\mathbf{Diff}_L$ (+0.64 °C/year), i.e the effect isopycnal diffusion, all the other terms tending to counter balance this warming. The strong additional warming from **ISO** to **ISOG** (+0.28 °C/year) is also only due to the added physics: the eddy-induced advection $\mathbf{Adv}_{EIV}$ adds 1.06 °C/year to the bowl, while the other terms (forcing and advection mostly) again tend to counter balance this effect (Table 1). After 40 years, the bowl heat budgets of **HOR**, **ISO** and **ISOG** exhibit the same relative balance between the trends as during the initial years (not shown) except that a quasi-equilibrium of T_{bowl} is reached for all 3 simulations ($\partial_t T_{bowl} \approx 0.01$ °C/year) due to a decrease of the forcing term. Hence, most of the conclusions regarding the behavior of the different lateral physics can be obtained from the first 3 years of simulation.

The time evolution of the monthly cumulated trends in this southern region (Fig. 7) vividly shows that the bowl temperature seems strongly dominated by the forcing. This is in agreement with the common idea that the mid-latitude ocean mixed layer is solely driven by air-sea fluxes. Nevertheless, in an annual mean sense, the forcing is not the dominant term as seen in Table 1. Furthermore, the seasonal cycle of T_{bowl}, entirely due to the forcing in **HOR** (Fig. 7-a), is modified by the added physics. The warming due to $\mathbf{Diff}_L$ in **ISO** (and to $\mathbf{Adv}_{EIV}$ in **ISOG**) is active all year long, but exhibit a marked maximum at the end of the winter, when the mixed-layer fully occupies the bowl (Fig. 7-b,c), i.e. when the ocean interior is in direct contact with the atmosphere *via* the mixed-layer (Fig. 7-b). The sign of

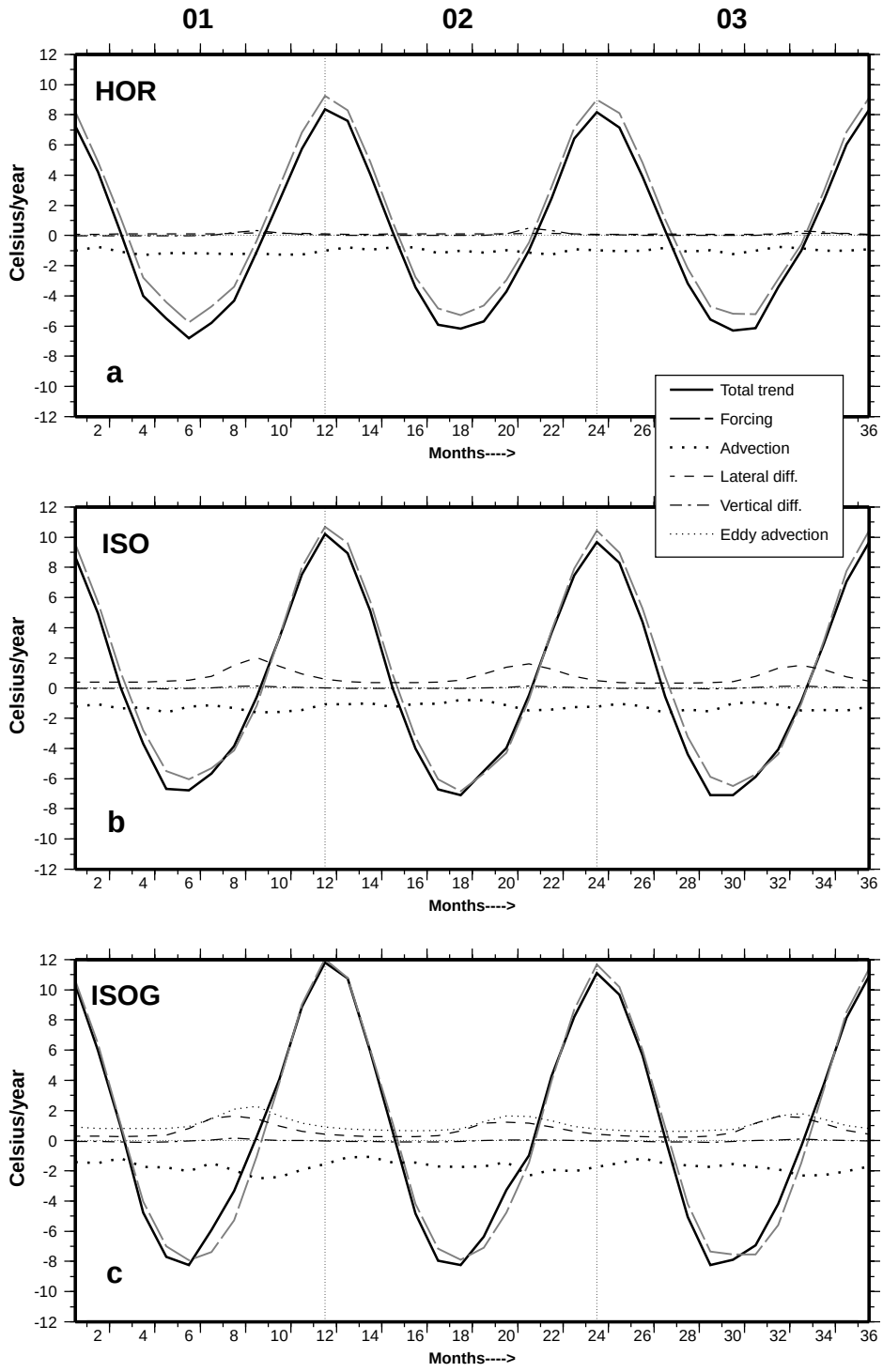

FIG. 7. *Monthly evolution of the bowl temperature trends at mid-latitudes in the southern Pacific (130°E-80°W/40°S-65°S) for years 01-02-03 (°C/year). (a) simulation **HOR**, (b) simulation **ISO** and (c) simulation **ISOG**.*

$\mathbf{Diff}_L$ in isopycnal diffusion indicates that the ocean interior is warming the bowl.

4.c The role of salinity in isopycnal mixing

Hirst and Cai (1994) qualitatively described such heat and salt exchanges between the subsurface and the mixed-layer in a forced isopycnal simulation. Understanding and quantifying this mixed-layer heating by $\mathbf{Diff}_L$ from the ocean interior in **ISO** requires to elucidate its *sign* and its increased *magnitude* when compared to $\mathbf{Diff}_L$ in **HOR**. The isopycnal diffusion trend $\mathbf{Diff}_L$ can be written as the product of the lateral diffusion coefficient K_L, the lateral gradient of temperature $\nabla_L T$ and the effective surface of lateral diffusion S_{eff} divided by the volume of the bow V:

$$\mathbf{Diff}_L = K_L \ \nabla_L T \ \ S_{eff}/V$$

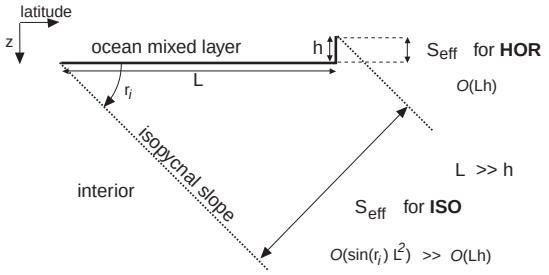

FIG. 8. *Definition of the effective surface of diffusion across the bowl, S_{eff}, for both horizontal and isopycnal diffusion operators.*

TABLE 2. Components of the isopycnal diffusion temperature trend $\mathbf{Diff}_L = K_L \nabla_L T \; S_{eff}/V$ *in the bowl of the southern ocean region drawn in Fig. 5. Mean values for year 01 of* ***HOR*** *and* ***ISO****, and ratio. See text for definitions. The order of magnitude between* $\mathbf{Diff}_{HOR}$ *and* $\mathbf{Diff}_{ISO}$ *is almost entirely due to the increase of the effective surface of lateral diffusion* S_{eff}.

	$1/V$ $10^{-15} m^3$	K_L $m^2 s^{-1}$	$\nabla_L T$ $10^{-5} \circ C\, m^{-1}$	S_{eff} $10^{10} m^2$
HOR	1/6.2	2.10^3	1.6	0.9
ISO	1/5.0	2.10^3	1.0	17
ratio **ISO** /**HOR**	1.2	1	0.6	19

We saw that $\mathbf{Diff}_{ISO}$ is one order of magnitude larger than $\mathbf{Diff}_{HOR}$ (Table 1). Table 2 shows the annual-mean components of $\mathbf{Diff}_L$ in the southern region of study for year 01 of **HOR** and **ISO**. The ratio $\mathbf{Diff}_{ISO}/\mathbf{Diff}_{HOR}$ is equal to 9.1 and is almost entirely due to the increased effective surface of lateral diffusion S_{eff}, which the perpendicular projection of the diffusion direction on the surface of the bowl. Indeed, in isopycnal diffusion, the *horizontal* surface of the ocean comes into play in S_{eff} (due to the slope of the isopycnals — Fig. 8). Because of the strong vertical/horizontal aspect ratio of the ocean, the surface of the vertical projection of the bowl is several orders of magnitude larger than its horizontal counterpart. This leverage effect is small in the tropics where the slope of the isopycnals is small but becomes quite important at mid-latitudes, explaining the magnitude of $\mathbf{Diff}_L$ there in **ISO**. The sign of $\mathbf{Diff}_L$ can be explained by looking at a "vertical" temperature section in the south Pacific, where depth is replaced by density (Fig. 9-a)*. This section, typical of the southern ocean structure, allows a clear view of *positive* isopycnal temperature gradients between the ocean interior and the bowl. For instance, at $\sigma_0 = 27.3$, the temperature just below the bowl is ~4°C while it is ~2°C inside the bowl (Fig. 9-a). Following the definition of an isopycnal (neutral surface), $\nabla_I T$ is proportional to $\nabla_I S$, where S is the salinity. This demonstrates the key role of salinity in isopycnal heat exchanges. Without salt, isopycnal mixing becomes isothermal, and the SST of **ISO** could not increase when compared to that of **HOR**. Around 40-60°S, where the maximum of $\mathbf{Diff}_L$ is seen in **ISO**, the surface salinity is quite low (Fig. 9-b) (precipitations and sea-ice cycle) while the salinity of the waters just below the bowl (further down the isopycnals) is higher, due to the advection of high salinity subtropical waters by the gyre (Fig. 9-b,c). Assuming $K_I = 10^3 m^2 s^{-1}$, Osborn (1997) estimated such isoneutral heat fluxes from the Levitus (1982) atlas to be of the order of *10* to *15* $W m^{-2}$ upwards at mid-latitudes, near the base of the bowl. He further shows that applying horizontal diffusion to the temperature field will generate a (spurious) diapycnal heat flux directed *downwards* in most of the ocean. These quite different effects of horizontal and isopycnal diffusion on the heat transfer near the base of the bowl are strikingly illustrated by contrasting Figs. 9-a and 9-c. In particular Fig. 9-c clearly shows the strong diapycnal component of horizontal diffusion, as well as a quite different direction of diffusion across the bowl.

4.d The eddy-induced advection effect

In **ISOG**, the warming of the bowl by $\mathbf{Adv}_{EIV}$ in the southern ocean region of study (Fig. 7-c) is due to the southward eddy-induced heat transport through the base of the bowl. As implied by Fig. 2-f (in particular by the position of the zero difference isocontour), more heat is transfered from lower to higher latitudes. Because of the particular shape of the bowl at the latitude of the region of study (downwards towards the south) and because of the existence of the isopycnal gradient of temperature described above, $\mathbf{Adv}_{EIV}$ is a positive contribution. In the mixed-layer, the individual eddy-induced and resolved-scale transports feature large and opposing heat transports (Gent and McWilliams 1996; Hirst and McDougall 1998). Table 1 allows to quantify the net heating due to these transports: in **ISOG**, $\mathbf{Adv}_{EIV}$ is warming the region of study by 1.06 °C/year while the resolved-scale advection (**Adv**) cools the region by 1.72 °C/year. The cooling by **Adv** is increased when compared to that of **ISO** (-0.47), but not enough to balance the eddy-induced warming (Table 1), evidencing the expected exagerated effect of the eddy-induced parameterization. This strong effect is most likely due to the high (and constant) value of K_{eiv} chosen. The strong southward eddy-induced heat transport in the mixed-layer contributes to the strong stratification seen at the base of the bowl (the vertical density gradient there is multiplied by 3 from **ISO** to **ISOG**).

* even though tracers are diffused along neutral density surfaces, potential density is a quite good approximation in the surface layers, particularly in the Pacific Ocean (You and McDougall 1990)

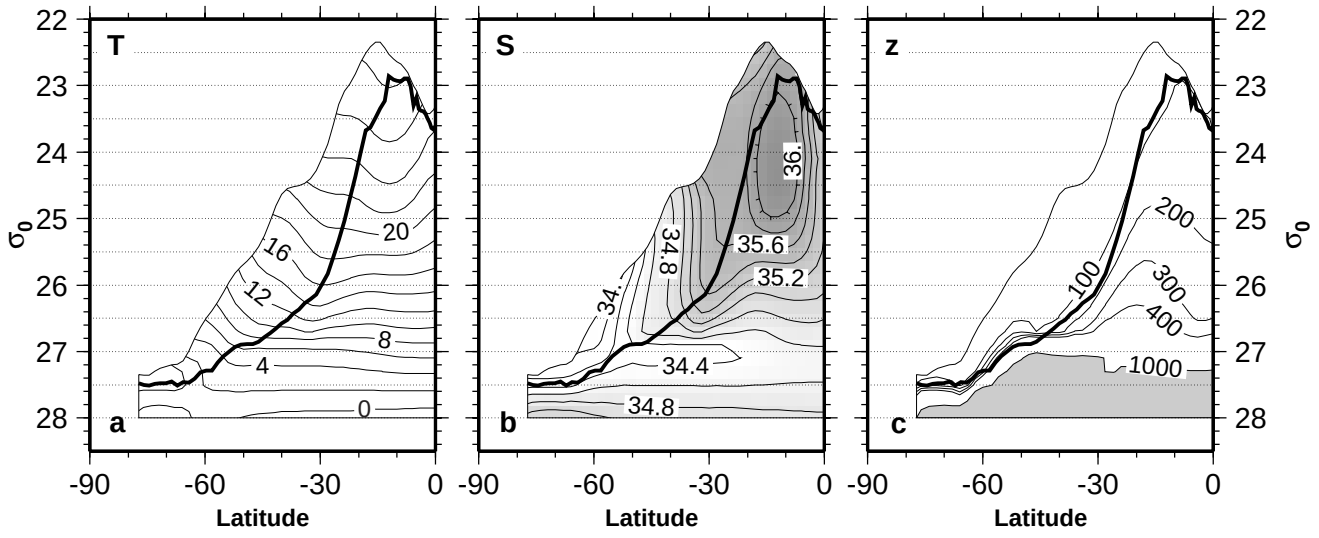

FIG. 9. *Latitude/potential density section at 160°E in the south Pacific for march 03 of simulation **ISO**. (a) temperature (°C), (b) salinity (PSU), (c) depth (m). The bowl of year 01-02-03 is denoted by a thick curve, the thin curve above it being the ocean surface.*

5. Discussion

5.a Climatic impacts

The changes of SST from one simulation to the other have non-negligeable impacts on the simulated climate. Global-mean SST differences of the order of 1°C after 40 years (Fig. 4) modified the air-sea heat fluxes (hence the top-of-the-atmosphere radiative balance) up to several watts per square meter. The sensitivity of the coupled system to the ocean physics is less spectacular than its sensitivity to atmosphere physics or resolution (Terray 1998, Madec and Delecluse 1997), but the choice of lateral ocean physics clearly plays a significant role in the adjustment of long-term climate simulations. Indeed, the rate at which water masses and thermocline waters are transformed affects the rate at which they are formed, hence the air-sea fluxes. The change in surface heat flux appears small when compared to present-day error bars in observed fluxes (1 or 2 $W\,m^{-2}$ versus 20 to 50 $W\,m^{-2}$), but one must keep in mind that the ocean *integrates* these differences (a heat flux of 1 $W\,m^{-2}$ applied to a 100m-deep mixed-layer raises its temperature by 1°C in 10 years). In addition, sensitivity experiments to doubling CO_2 (Cubash *et al.* 1992, Mitchell *et al.* 1995, Barthelet *et al.* 1998), show changes of SST and air-sea fluxes of the same order of magnitude as the ones seen in the present sensitivity experiment. As mentioned by McDougall *et al.* (1996), the ocean intake of heat is quite dependent on the ocean mixing parameterisation.

The "equivalent resistivity" of the bowl, which measures the resistance of the mixed-layer to an atmospheric warming Q_W can be associated to an "equivalent heat transfer coefficient" $\mathbf{K}_{tr}$ defined by the relation:

$$Q_W = \rho_0 C_p \mathbf{K}_{tr} \frac{\langle Ta_{2m} \rangle - \langle T_{bb} \rangle}{\langle H_b \rangle}$$

where Ta_{2m} is the 2 m air temperature, T_{bb} is the temperature at the base of the bowl, H_b is the depth of the bowl, ρ_0 is a reference density, C_p the specific heat of sea water and where $\langle \bullet \rangle$ indicates a global horizontal average. From $\mathbf{K}_{tr}$, we can define a characteristic time of heat transfer $\tau_{th} = \langle H_b \rangle^2 / \mathbf{K}_{tr}$. The values of τ_{th} computed for years 39-40 (after the initial adjustment phase of the upper ocean) for simulations **HOR**, **ISO** and **ISOG** are 30, 34 and 55 years, respectively. This indicates that the equivalent resistivity of the bowl increased by 10% from **HOR** to **ISO** and further by 60% from **ISO** to **ISOG**. We have seen in section 4 that in **ISO**, additional heat was transported from the ocean interior to the bowl (when compared to **HOR**) hence increasing the characteristic time of *net* heat transfer between the diabatic part of the ocean and the adiabatic part. In **ISOG**, even more heat is given back by the ocean interior to the bowl, hence the reduced global heat intake. One might further wonder how would the bowl equivalent resistivity respond to a global *cooling* due to air-sea fluxes, rather than the warming seen here. The compared response of the 3 physics is likely to be somewhat different as the dynamics of the mixed layer under cooling (destabilizing effect) is quite different than the one under warming (stabilizing effect). In the Northern Hemisphere, the net flux entering the ocean is negative (Fig. 3-a) even though still warmer than observed. Nevertheless, the upper ocean dynamics and thermodynamics are

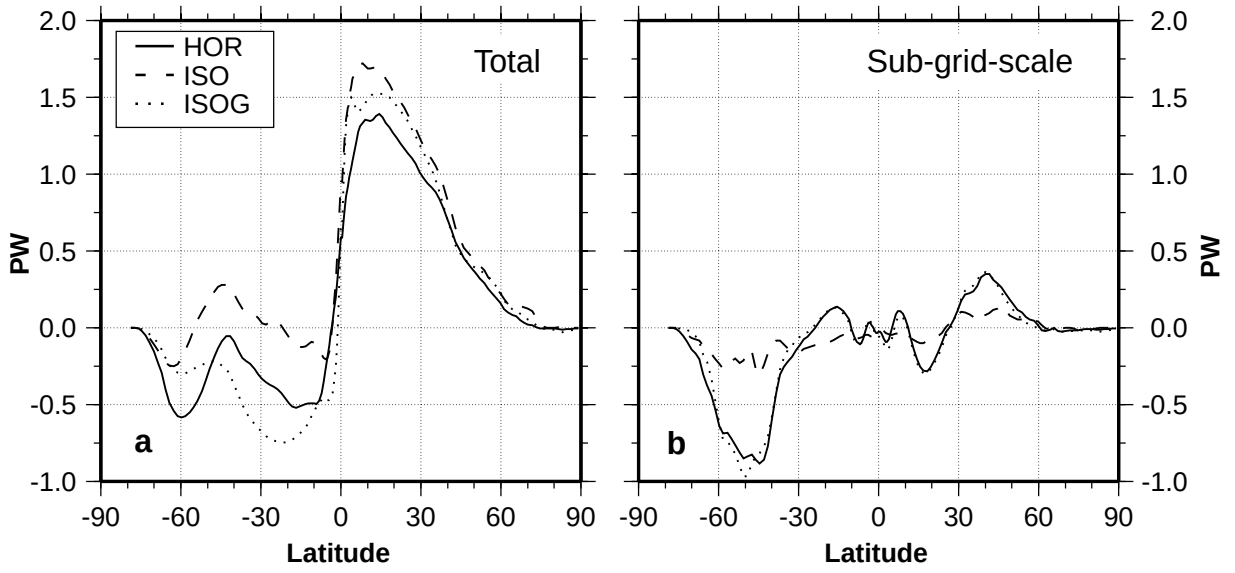

Fig. 10. *Meridional heat transport in the ocean (PW). Average of years 26-40 for the 3 simulations: (a) total transport, (b) transport due to sub-grid-scale processes.*

significantly complicated by the gyre circulation in both the North Pacific and the North Atlantic. Hence the heat balance of the bowl in the north is quite difficult to compare to the heat balance of the bowl of southern region previously discussed. A serie of coupled simulations exhibiting a surface cooling *over the southern ocean* would therefore be needed to conclude on that specific point.

The total heat transport in the southern hemisphere exhibits marked differences between the three simulations (Fig. 10-a). In **ISO**, as no background K_H is used, the diapycnal mixing is very small and the SGS contribution to the heat transport across the Antarctic Circumpolar Current (ACC) is strongly reduced when compared to that of **HOR** (Fig. 10-b). The consequence is that, even though **ISO** has an ocean density structure in better agreement with the initial state (it was not diffused away as in **HOR**), it has an unrealistic* total meridional heat transport in the southern hemisphere (Fig. 10-a). In the real world, eddies play a important role in transfering heat across the ACC. Indeed, adding an eddy-induced velocity increases the SGS heat transport across the ACC in **ISOG** (Fig. 10-b)** and the total heat transport is now again poleward in the southern hemisphere (Fig. 10-a). Moreover this is now achieved without the strong diffusive bias of **HOR**.

5.b GM90

The implementation of the eddy-induced velocity proposed by Gent and McWilliams (1990) degraded the thermodynamical structure of the upper ocean in the present coupled model. This result is in contrast with previous studies made in forced mode (Danabasoglu and McWilliams 1995, Hirst and McDougall 1996, McDougall *et al.* 1996). Several reasons can be invoqued: 1/ the air-sea interface of a coupled model is free and new water masses (due to deficients air-sea fluxes) are formed more easily than in a forced model (see analysis of present **ISO** and **ISOG** simulations by Speer *et al.* 1999); 2/ the K_{eiv} coefficient used here is twice the value used in these earlier studies and is constant; 3/ the result is compared to a "pure" isopycnal simulation (Weaver and Eby 1997 have shown that part of the improvement seen in these earlier studies came from the possibility of removing the background horizontal diffusion); 4/ the choice of the GM90 formulation both near the surface and at the bottom of the mixed-layer. This last point raises the issue of the choice of the boundary condition of GM90 in the mixed-layer, where the slope of the isopycnals is infinite (Tréguier *et al.* 1997, Tandon and Garrett 1996, Marshall 1997).

By breaking the classical "all fickian" lateral diffusion approach, thus allowing a non diffusive SGS transport across horizontal gradients (ACC), the physics addressed by GM90 is novel and promising (McDougall and McIntosh 1996, Killworth 1997). In the present study, the ocean heat transport in **ISOG** is improved in the southern hemisphere when compared to the one of **ISO** (Fig. 10-a). Nevertheless, the high and constant K_{eiv} and the surface boundary condition chosen here (so that the simulations could be compared) led to a rather extreme case of eddy advection.

5.c Interaction between physical parameterisations

Even though vertical and lateral mixing parameterisations are distinct, they both act to transform water

* at least with the present atmosphere GCM physics

** The meridional heat transport due to the eddy-induced advection has the same magnitude and latitudinal distribution as the SGS transport in **HOR** (Figure 10). This is due to the distribution of latitudinal temperature gradients and the equivalence of the two parameterisations was shown by Lazar *et al.* (1999).

masses. Hence, a change in one of the two is likely to affect the other. This was clearly shown by Maes *et al.* (1997) in the tropics where decreasing the horizontal eddy viscosity and diffusivity coefficients led to an increase of the corresponding vertical coefficients and significant changes in the equatorial circulation. In the present study, this direct link between lateral and vertical mixing is straightforward when using Walin (1982) approach. In **HOR**, both horizontal and vertical mixing participate to water-mass transformation (through diapycnal mixing). In **ISO**, the lateral mixing is *isopycnal* and the only source of *diapycnal* mixing (away from the surface layers) is the vertical mixing scheme. As a consequence, this mixing increases to take over the diapycnal exchanges performed by the horizontal operator in **HOR**. For instance, in the ocean interior of the northern hemisphere, the mean vertical diffusion coefficient in the thermocline ($25. < \sigma_0 < 27.$) went from $0.18\,10^{-4}\,m^2 s^{-1}$ in **HOR** up to $0.25\,10^{-4}\,m^2 s^{-1}$ in **ISO**, hence an increase of 40%.

A second type of interaction between parameterisations was seen in the southern ocean, where a change of ocean physics evidenced a physical deficiency in the atmospheric boundary layer (higher-than-observed heat fluxes). Indeed, improving the physics of the ocean degraded the SST in the southern ocean: in **HOR** the spurious excess of heat entering the mixed layer made its way towards the interior of the ocean faster than in **ISO** or **ISOG** (due to the weaker equivalent resistivity of the bowl). The added physics in **ISO** and **ISOG** increased the equivalent resistivity of the bowl and trapped the additional heat coming from the atmosphere GCM in the ocean surface layers. The subsequent increase of SST in turn modified the heat fluxes computed by the atmosphere GCM (decrease of the latent heat flux). But this change does not necessarily have an effect on the deficient parameterisation (clouds) in this region. This is an intricate coupled problem between ocean and atmosphere GCM parameterisations and should be tackled as such (Terray 1998).

6. Conclusion

The sensitivity of the upper ocean thermal balance of a coupled ocean-atmosphere GCM to ocean lateral physics is addressed. Three 40-year coupled simulations are made using the OPA/OASIS/ARPEGE model: **HOR** with horizontal diffusion, **ISO** with isopycnal diffusion and **ISOG** with isopycnal diffusion plus an eddy-induced advection (GM90). In response to the change of ocean physics, the air-sea heat exchanges are modified by several $W\,m^{-2}$ (further modifying the top-of-the-atmosphere radiative balance). This confirms the central role of ocean turbulence in the climate system: the rate at which water masses and thermocline waters are transformed affects the rate at which they are formed (Walin 1982), hence the air-sea fluxes. The initial adjustment phase of the SST is used to diagnose the physical mechanisms involved in each parameterisation. When the lateral ocean physics is modified, significant changes of SST are seen at mid-latitudes, in particular in the southern ocean. An excess of heat entering the ocean there is originally due to larger-than-observed atmospheric heat fluxes generated by the atmosphere GCM in this region. In **HOR**, this warming is diffused away in the ocean interior while part of it is given back to the mixed-layer when new lateral physics are added. A measure of the rate of ocean heat intake is derived as an "equivalent resistivity of annual mixed-layer". From **HOR** to **ISO** and further to **ISOG**, this resistivity increases and the associated characteristic times of heat transfer are 30, 34 and 55 years, respectively.

The use of an isopycnal mixing scheme (applied with no horizontal background diffusion) improves the ocean climatology when compared to that of **HOR**. The isopycnal scheme modifies the heat input from the mixed-layer into the ocean interior and is therefore directly responsible for the southern ocean SST increase seen from **HOR** to **ISO**. The physical mechanism responsible is a positive heat flux from the ocean interior into the mixed-layer. It is both due to an increased effective surface of diffusion across the base of the annual mixed-layer (defined as the bowl) and to the sign of the isopycnal gradients of temperature. As isopycnal gradients of temperature are proportional to isopycnal gradients of salinity, this demonstrates a quite strong role of salinity in the heat balance of climate. Indeed, as shown in this paper, the salinity structure strongly participates to the thermal consumption of the ocean (especially at mid-latitudes) and therefore to the heat exchanges between the ocean and the atmosphere. This result is all the more interesting as the surface coupling of salt and fresh water is quite weak when compared to that of SST and heat fluxes, allowing complex feedbacks yet to be explored.

The eddy-induced advection also leads to increased exchanges between the bowl and the ocean interior. This is both due to the shape of the bowl and again to the existence of a salinity structure. The corresponding strong advective heat transfert from the ocean interior towards the bowl reduces the heat intake of the ocean interior. This effect is too strong as adding the GM90 eddy-induced velocity degrades the upper-ocean structure when compared to that of **ISO**. The choice of a strong and constant eddy-induced coefficient plus the particular boundary conditions chosen in the mixed-layer led to a rather extreme case of the parameterization. An intense surface poleward heat transport led to a strong stratification at the base of the mixed-layer. Nevertheless, by allowing non-diffusive sub-grid-scale transport across horizontal gradients, the eddy-induced velocity improves the meridional heat transport in the southern ocean, when compared to that of the isopycnal-only simulation. Eddies play an important role in transporting

heat across the ACC. Here, this effect is exagerated by the particular set-up of GM90 chosen. The real transport is probably in between that of **ISO** and **ISOG** (Speer *et al.* 1999).

The lateral ocean physics is therefore shown to be a main contributor to the exchanges between the diabatic and the adiabatic parts of the ocean (with the same magnitude as the vertical ocean physics). Hence its central climatic role, both due to a control of the heat intake capacities of the ocean and to its ability to extract long term memory from the ocean interior towards the warm sphere of the coupled ocean-atmosphere system.

This study of the ocean physics in coupled mode was fruitful: the SST warming in the south was seen thanks to the use of a coupled model without any artificial flux corrections (upper boundary of the mixed layer not constrained) and without any ocean thermodynamical spin-up. In forced mode, the physical mechanisms described above do exist but their effects on the SST are offset by the surface feedback term. Of course, this feedback term is slightly different with different lateral physics but the physical interpretation of these changes is unclear. Nevertheless, relaxing the air-sea interface constraint multiplies the degrees of freedom of the modeled system, hence its complexity. In particular, the strong interactions between the different physical parameterisations (both within each model and between models, and especially between the two surface boundary layers) advocate for their parallel development, improving the weak link in the physics of the ensemble rather than just one parameterisation. In particular, one should avoid "tuning" a parameterisation to obtain a *global* realistic climatology as this will often result in error compensations and will eventually jeopardize subsequent model improvements.

The analysis of the initial adjustment phase of the upper ocean yielded many results on the effect of the 3 physical parameterisations used. Hence, driving an ocean model to a thermodynamical equilibrium is not a prerequisite to understand the behavior of its underlying physics. This initial adjustment approach can therefore be quite useful to improve short coupled simulations (eddy-resolving models, seasonal prediction models,...).

The mid-latitudes atmosphere - ocean interior connection due to isopycnal diffusion is found all year round but has a marked maximum at the end of the winter, modifying the strong seasonal cycle of temperature there, mostly driven by forcing. This could allow a participation of the ocean interior to the low-frequency variability of the coupled system at these latitudes. In addition, as in isopycnal diffusion the salinity is now an active component of the circulation at all latitudes, it is expected that the variability of the coupled system will be quite dependent on the lateral ocean physics chosen. This issue will be addressed in a subsequent paper.

Acknowledgments: We especially thank Kevin Speer, Olivier Thual, Pascale Delecluse, Jean-François Minster and David Marshall for helpful discussions. Maurice Imbard and Michel Déqué provided the ocean and atmosphere GCMs. Jérome Vialard helped with the computation of the trends in OPA8. We thank two reviewers for helpful comments that led to improvements of the original manuscript. This work was partially supported by EEC contract ENV4-CT95-0102 SIDDACLICH and by Programme National d'Étude du Climat (PNEDC). Computations were carried out at the computing centers of Météo-France and IDRIS/CNRS.

REFERENCES

Barthelet, P., L. Terray, and S. Valcke, 1998 : Transcient CO2 experiment using the ARPEGE/OPAICE non-flux corrected coupled model. *Geophys. Res. Letters*, *25-13*, 2277-2280.

Blanke, B., and P. Delecluse, 1993 : Variability of the tropical atlantic ocean simulated by a general circulation model with two different mixed layer physics. *J. Phys. Oceanogr., 23*, 1363-1388.

Caldwell, D. R., and J. N. Moum, 1995: Turbulence and mixing in the ocean. *Rev. Geophys.*, 13855-1394.

Cox, M. D., 1987: Isopycnal diffusion in a z-coordinate ocean model. *Ocean Modelling*, 74, 1-9.

Cubasch, U., K. Hasselmann, H. Hock, E. Maier-Reimer, U. Mikolajewicz, B. D. Santer, and R. Sausen, 1992: Time-dependent greenhouse warming computations with a coupled ocean-atmosphere model. *Climate Dyn., 8*, 55-69.

Danabasoglu, G., and J. C. McWilliams, 1995 : Sensitivity of the global ocean circulation to parameterizations of mesoscale tracer transports. *J. Climate*, 8, 2967-2987.

Dandin, P., and J.-J. Morcrette, 1996: The ECMWF FMR scheme in the Météo-France climate model ARPEGE-Climat, Note 50, CNRM, France, 74pp.

Déqué, M., C. Dreveton, A. Braun, and D. Cariolle, 1994: The climate version of Arpège/IFS: a contribution to the French community climate modelling. *Clim. Dyn., 10*, 249-266.

England, M. H., 1993: Representing the global-scale water masses in ocean general circulation models. *J. Phys. Oceanogr, 23*, 1523-1552.

England, M. H., and A. C. Hirst, 1997: Chlorofluorocarbon in a world ocean model. Part 2. Sensitivity to surface thermohaline forcing and subsurface mixing parameterizations. *J. Geophys. Res, 102*, 15,709-15,731.

Gargett, A. E., 1989 : Ocean turbulence. *Ann. Rev. Fluid Mech.*, 21, 419-452.

Gent, P. R., and J. C. McWilliams, 1990: Isopycnal mixing in ocean circulation models. *J. Phys. Oceanogr., 20*, 150-155.

Gent, P. R., and J. C. McWilliams, 1996: Eliassen-Palm fluxes and momentum equation in non-eddy-resolving ocean circulation models. *J. Phys. Oceanogr., 26*, 2539-2546.

Gent, P. R., J. Willebrand, T. J. McDougall, and J. C. McWilliams, 1995: Parameterizing eddy-induced tracer transports in ocean circulation models. *J. Phys. Oceanogr., 25*, 463-474.

Guilyardi, E., and G. Madec, 1996 : Climatology of the OPA-ARPEGE intermediate resolution coupled ocean-atmosphere model.*Clim.Dyn., 13,* 149-165.

Guilyardi, E., 1997: Rôle de la physique océanique sur la formation/consommation des masses d'eau dans un modèle couplé océan-atmosphère. PhD thesis, Université Paul Sabatier, Toulouse, France, 195pp.

Hirst, A. C., and W. Cai, 1994: Sensitivity of a world ocean GCM to changes in subsurface mixing parameterization. *J. Phys. Oceanogr., 24,* 1256-1279.

Hirst, A. C., and T. J. McDougall, 1996: Deep-water properties and surface buoyancy flux as simulated by a z-coordinate model including eddy-induced advection.*J. Phys. Oceanogr., 26,* 1320-1343.

Killworth, P. D., 1997: On the parameterization of eddy transfer. Part I: Theory. *J. Mar. Res., 55,* 1171-1197.

Large, W. G., J. C. McWilliams, and S. C. Doney, 1994: Oceanic vertical mixing: a review and a model with a nonlocal boundary layer parameterization. *Rev. Geophys., 32,* 366-403.

Lazar, A., G. Madec, and P. Delecluse, 1998: A rationalization of the Veronis upwelling / downwelling system and its sensitivity to mixing parameterizations in an idealized OGCM. *J. Phys. Oceanogr.*, in press.

Ledwell, J. R., A. J. Watson, and C. S. Law, 1997: Mixing of tracer in the pycnocline *Nature, 364,* 701-703.

Ledwell, J. R., A. J. Watson, and C. S. Law, 1993: Evidence for slow mixing across the pycnocline from an oipen-ocean tracer-release experiment. *Nature, 364,* 701-703.

Ledwell, J. R., A. J. Watson, and C. S. Law, 1998: Mixing of tracer in the pycnocline *J. Geophys. Res., 103,* 21,499-21,529.

Levitus S., 1982: *Climatological atlas of the Word Ocean.* NOAA Prof. Paper No. 13., U.S. Govt. Printing Office, Washington D.C., 173pp and 17 microfiches.

Luyten, J. R., J. Pedlosky and H. Stommel, 1983: The ventilated thermocline. *J. Phys. Oceanogr., 13, 292-309*.

Madec, G. and P. Delecluse, 1997: The OPA/ARPEGE and OPA/LMD Global Ocean-Atmosphere Coupled Model. *Int. WOCE Newsletter, 26,* 12-15.

Madec, G., and M. Imbard, 1996: A global ocean mesh to overcome the North Pole singularity. *Clim.Dyn., 12,* 381-388.

Madec, G., P. Delecluse, M. Imbard, and C. Lévy, 1998: OPA 8.1 Ocean General Circulation Model reference manual. *Note du Pôle de modélisation,* Institut Pierre-Simon Laplace, *N°11,* 91pp.

Maes C., G. Madec and P. Delecluse, 1997: Sensitivity of an Equatorial Pacific OGCM to the lateral diffusion. *Mon. Wea. Rev., 125,* 5, 958-971.

Marshall, J. C., and A. J. G. Nurser, 1992: Fluid dynamics of oceanic thermocline ventilation. *J. Phys. Oceanogr., 22,* 583-595.

Marshall, D., 1997: Subduction of water masses in an eddying ocean. *J. Mar. Res., 55,* 201-222.

McDougall, T. J., and P. C. McIntosh, 1996: The temporal-residual-mean velocity: I derivation and scalar conservation equations. *J. Phys. Oceanogr., 26,* 2653-2665.

McDougall, T. J., A. C. Hirst, M. H. England, and P. C. McIntosh, 1996: Implications of a new eddy parameterization for ocean models. *Geophys. Res. Let., 23,* 2085-2088.

McDougall, T. J., 1987: Neutral surfaces. *J. Phys. Oceanogr., 17,* 1950-1964.

McWilliams, J. C., 1996: Modelling the oceanic general circulation. *Ann. Rev. Fluid Mech., 28,* 215-248.

Mitchell, J. F. B., T. C. Johns, J. M. Gregory, and S. F. B. Tett, 1995: Climate response to increasing levels of greenhouse gases and sulphate aerosols. Nature, *376,* 501-504.

Osborn, T. J., 1997: The vertical component of epineutral diffusion and the dianeutral component of horizontal diffusion. *J. Phys. Oceanogr., in press.*

Polzin, K. L., K. G. Speer, and J. M. T. R. W. Schmitt, 1996: Intense mixing of Antarctic Bottom Water in the equatorial Atlantic Ocean. *Nature, 380,* 54-57.

Polzin, K. L., J. M. Toole, J. R. Ledwell, and R. W. Schmitt, 1997: Spatial variability of turbulent mixing in the abyssal ocean. *Science, 276,* 93-96.

Redi, M. H., 1982: oceanic isopycnal mixing by coordinate rotation. *J. Phys. Oceanogr., 13,* 1154-1158.

Rhines, P. B., and W. R. Young, 1982: A theory of the winf-driven circulation. *J. Mar. Res, 40,* 559-596.

Speer, K., E. Guilyardi, and G. Madec, 1999: Southern ocean transformation in a coupled model with and without eddy mass fluxes. *Tellus*, submitted.

Tandon, A., and C. Garrett, 1996: On a recent parameterization of mesoscale eddies. *J. Phys. Oceanogr., 26,* 406-411.

Terray, L., 1996: The OASIS coupler user guide, version 2.1. Tech. Rep. TR/CMGC/96-46, CERFACS, France.

Terray, L., 1998: Sensitivity of climate drift to atmospheric physical parameterizations in a coupled ocean-atmosphere general circulation model. *J. Climate*, 11, 1633-1658.

Toole, J. M., K. L. Polzin, and R. W. Schmitt, 1994: New estimates of diapycnal mixing in the abyssal ocean. *Science, 264,* 1120-1123.

Tréguier, A.-M., I. M. Held, and V. D. Larichev, 1997: Parameterization of quasi-geostrophic eddies in primitive equation ocean models. *J. Phys. Oceanogr., 27,* 567-580.

Tziperman, E., 1986: On the role of interior mixing and air-sea fluxes in determining the stratification and circulation of the oceans. *J. Phys. Oceanogr., 16,* 680-693.

UNESCO, 1983: Algorithms for computation of fundamental property of sea water. *UNESCO Techn. Paper in Mar. Sci.*, 44, Unesco, 53pp.

Visbeck, M., J. Marshall, T. Haines, and M. Spall, 1997: On the specification of eddy transfert coefficients in coarse-resolution ocean circulation models. *J. Phys. Oceanogr., 27,* 381-402.

Walin, G., 1982: On the relation between air-sea heat flow and thermal circulation in the ocean. *Tellus, 34,* 187-195.

Weaver, A. J., and M. Eby, 1997 : On the numerical implementation of advection schemes for use in conjuction with various mixing parameterizations in the GFDL ocean model. *J. Phys. Oceanogr., 27,* 369-377.

You, Y., and T. J. McDougall, 1990: Neutral surface and potential vorticity on the wold's oceans. *J. Geophys. Res., 95-C8,* 13,235-13,261.